

Supporting Information for

## Hierarchical Bi<sub>2</sub>MoO<sub>6</sub> Nanosheet-Built Frameworks with Excellent Photocatalytic Properties

Ying Ma,<sup>a,b</sup> Yulong Jia,<sup>a,b</sup> Zhengbo Jiao,<sup>a</sup> Min Yang,<sup>a</sup> Yanxing Qi,<sup>a,\*</sup> and Yingpu Bi<sup>a,\*</sup>

<sup>a</sup> State Key Laboratory for Oxo Synthesis & Selective Oxidation, and National Engineering Research Center for Fine Petrochemical Intermediates, Lanzhou Institute of Chemical Physics, CAS, Lanzhou 730000, China.

Email: [yingpubi@licp.cas.cn](mailto:yingpubi@licp.cas.cn); [qiyx@lzb.ac.cn](mailto:qiyx@lzb.ac.cn)

<sup>b</sup> University of Chinese Academy of Sciences, Beijing 100049, China.

### Experimental Section

#### 1. Synthesis of MoO<sub>3</sub> nanobelts

All chemical reagents were analytical grade and used as-received. The molybdenum trioxide nanobelts were prepared by the hydrothermal method described in ref 1. As typically, 20 ml of 30 wt% H<sub>2</sub>O<sub>2</sub> aqueous solution was slowly added to 2.4 g Mo metal powder in an icy water bath with magnetic stirring. After about 3 h, a transparent yellow solution was obtained, and then diluted into 250 ml solution. In order to synthesis of MoO<sub>3</sub> nanobelts, 60 ml of precursor solution was sealed in a 150 ml autoclave and hydrothermally treated at 180 °C for 24 h.

#### 2. Synthesis of Bi<sub>2</sub>MoO<sub>6</sub> nanosheet-built frameworks

The synthesis of Bi<sub>2</sub>MoO<sub>6</sub> nanosheet frameworks were performed via a simple reflux process, in which 0.7 mmol obtained molybdenum trioxide nanobelts and 1.4 mmol bismuth nitrate were dissolved in 20 ml deionized water and refluxed in oil bath at 120 °C for 2 h, 4 h, 6 h and 8 h, respectively. After the solution cooling down to room temperature, the prepared products were centrifuge separated with solvent and washed three-times with deionized water and ethanol, respectively, followed by drying in a vacuum oven at 60 °C for overnight. For comparison, Bi<sub>2</sub>MoO<sub>6</sub> particles (BMNP) were prepared by a traditional solid-state reaction shown in ref 2 and Bi<sub>2</sub>MoO<sub>6</sub> nanosheets (BMNS) were synthesized by the hydrothermal method described in ref 3.

#### Reference

1. L. Zhou, L.C. Yang, P. Yuan, *J. Phys. Chem. C*, 2010, **114**, 21868–21872.
2. K.M. Chanapa, M. Vladimir, *Cryst. Growth Des.*, 2012, **12**, 5994–6003.
3. C. Xu, D.B. Zou, L.H. Wang, *Ceramics International*, 2009, **35**, 2099–2102.

#### 3. Photocatalytic Reactions

In the photocatalytic activity of experiments, the samples (0.02 g) were put into a solution of Rhodamine B (RhB) dyes (20 ml, 10<sup>-5</sup> mol/L), which was then irradiated with a 300W Xe arc lamp equipped with an ultraviolet cutoff filter to provide visible light with  $\lambda \geq 420$  nm. The degradation of RhB was monitored by UV/Vis spectroscopy (UV-2550, Shimadzu). Before the spectroscopy measurement, these photocatalysts were removed from the photocatalytic reaction systems by a dialyzer. The photocatalytic activity of the product is evaluated by the decomposition of RhB under visible light irradiation. Temporal changes in the concentration of RhB, as monitored by the maximal absorption of RhB at 554 nm in the UV-vis spectra over the as-prepared photocatalysts, are shown in Fig. S7. Moreover, the BMNP, BMNS and Degussa-P25 samples are used as photocatalytic references for comparison with the HBNF. The degradation efficiency of all the samples is defined as  $C/C_0$ , where  $C$  and  $C_0$  represent the remnant and initial concentration of RhB, respectively. Before the photocatalytic experiments, the reaction solutions containing

catalysts were kept in the dark for 30 min to reach the adsorption-desorption equilibrium. In the case of the phenol degradation, the experimental conditions are same as the RhB degradation except for the amounts of catalysts (0.05 g) and concentrations of phenol aqueous solution (50 ml,  $10^{-4}$  mol/L).

#### 4. Photoelectric conversions

The photoelectric conversion properties were investigated in a conventional three-electrode cell by using computer-controlled electrochemical workstation (CHI 660D). 50 mg catalysts were suspended in 2 mL water, the mixtures were ultrasonically scattered for 15 min to form homogeneous solution. Then, 0.1 mL solution was dropped on the Fluorine doped tin oxide (FTO) glass (1×2 cm). After evaporation of the water in air, the catalyst was attached onto the surface of FTO glass. A Pt wire, saturated calomel electrode (SCE), and 0.1 M sodium sulfate were used as the working electrode, the counter-electrode, the reference electrode, and the electrolyte, respectively. The current-time (*i-t*) curves were collected at 1 V vs SCE. The light source was a 300W Xe lamp, and a cutoff filter of 420nm was employed for the visible-light irradiation.

#### 5. Characterizations

SEM images were taken using a field-emission scanning electron microscope (JSM-6701F, JEOL) operated at an accelerating voltage of 5 kV. TEM images were carried out by using an FEI Tecnai TF20 microscope operated at 200 kV. The X-ray diffraction spectra (XRD) measurements were performed on a PANalytical X'pert PRO instrument using Cu K $\alpha$  radiation (40 kv). The XRD patterns were recorded from 10° to 80° with a scanning rate of 0.067°/s. UV/Vis absorption spectra were taken at room temperature on a UV-2550 (Shimadzu) spectrometer. The oxidation states of the product were investigated through an ESCALAB 250 X-ray photoelectron spectrometer (XPS) with non-monochromatized Mg K $\alpha$  X-ray as excitation source. Specific surface area of samples was measured with a ASAP 2020M instrument and analyzed by the Brunauer-Emmett-Teller (BET) equation. The pore size distribution plots were obtained by the Barret-Joyner-Halenda (BJH) model.

## Additional Figures and Discussions

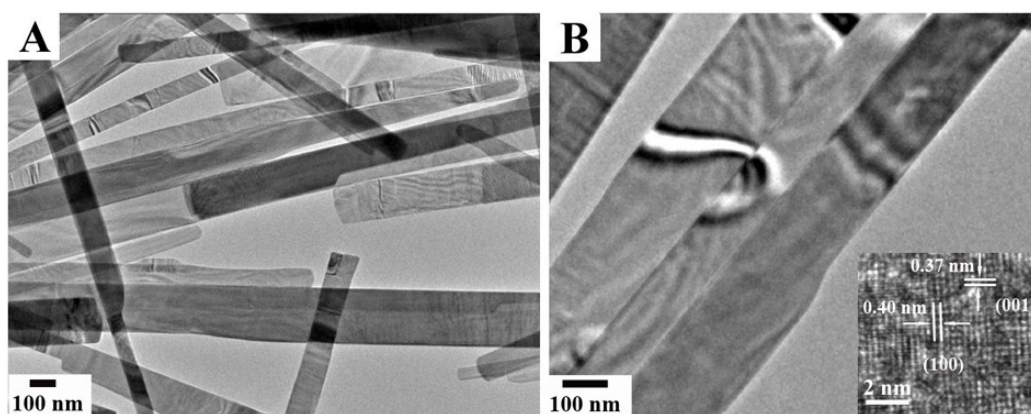


**Fig. S1.** TEM images of the obtained MoO<sub>3</sub> nanobelts by a hydrothermal reaction.

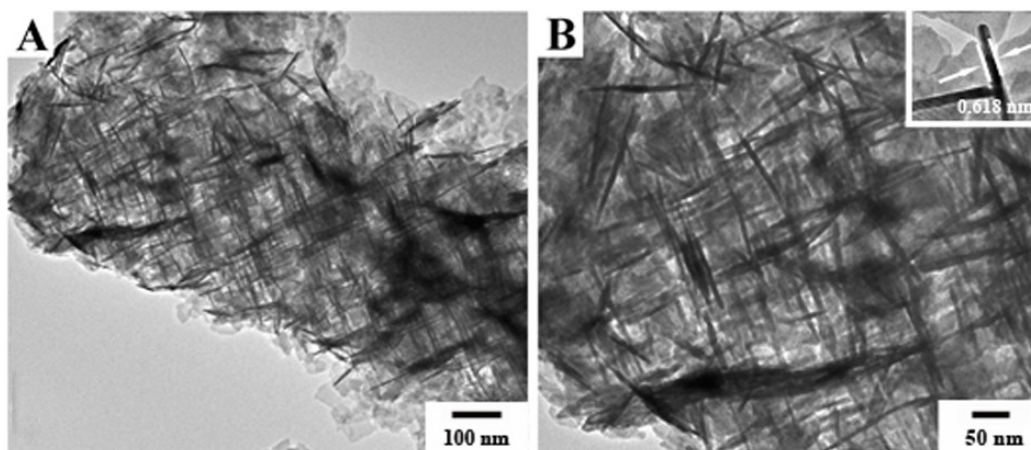


**Fig. S2.** TEM images of the obtained hierarchical Bi<sub>2</sub>MoO<sub>6</sub> nanosheet framework (HBNF) with different resolution.

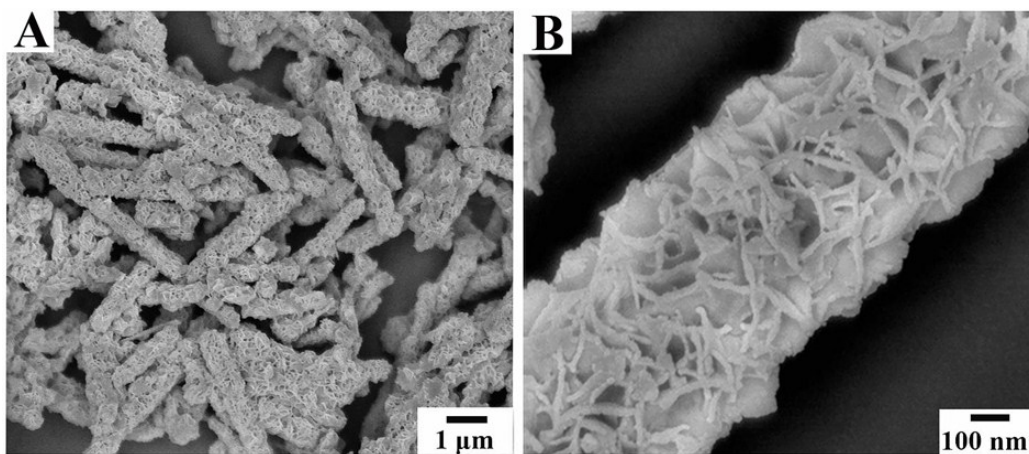


**Fig. S3.** SEM image (A) and (B) of the obtained hierarchical  $\text{Bi}_2\text{MoO}_6$  nanosheet framework (HBNF) refluxed at  $120^\circ\text{C}$  for 8 h.

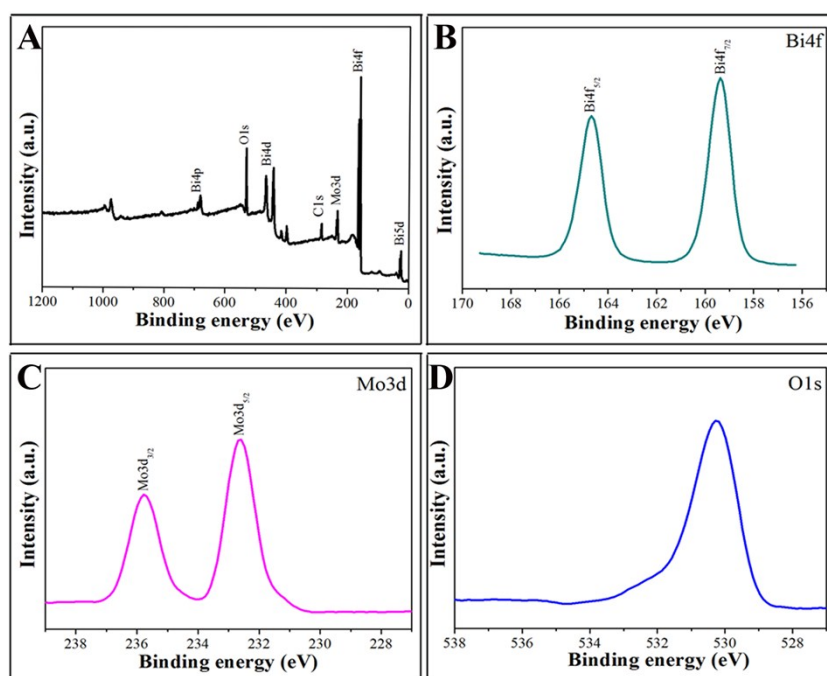


**Fig. S4.** XPS spectra (A) survey spectrum, (B) Bi 4f, (C) Mo 3d, (D) O 1s of one-dimensional  $\text{Bi}_2\text{MoO}_6$  nanosheet framework (HBNF) obtained by a reflux reaction.

In order to investigate the composition of the product and valence state of the individual element, the as-obtained product was further investigated by XPS. The XPS of the sample shows the main peaks of Bi4f, Mo3d, O1s and Cl1s. Fig. S4B shows the high-resolution XPS of Bi4f. Two peaks with the binding energies of 159.05 eV and 164.4 eV, representing  $\text{Bi}4f_{7/2}$  and  $\text{Bi}4f_{5/2}$  electrons, respectively, are corresponded to Bi (III) according to the literatures.<sup>4</sup> As for Fig. S4C, the binding energies at around 232.2 eV and 235.8 eV can be ascribed to Mo 3d. In the O1s pattern (Fig. S4D), the peak at 530.9 eV is ascribed to the Bi-O bonds in  $\text{Bi}_2\text{MoO}_6$ .<sup>5</sup>

#### Reference

4. H.B. Lu, S.M. Wang, L. Zhang, *J. Mater. Chem.*, 2011, **21**, 4228–4234.
5. Y.S. Xu, W. D. Zhang, *Dalton Trans.*, 2013, **42**, 1094–1101.

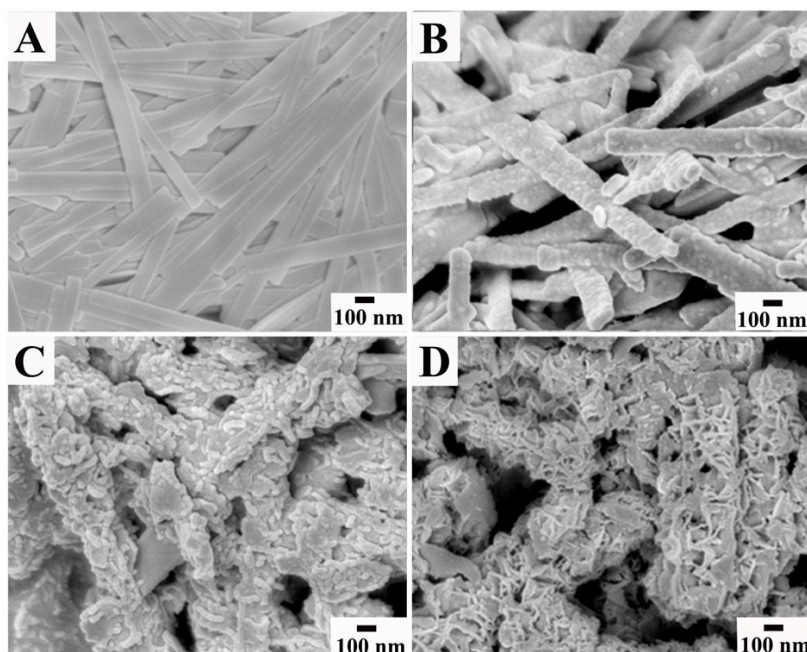


**Fig. S5.** SEM images of the intermediates collected after the reflux reaction had processed for (A) 0 h, (B) 2 h and (C) 4 h, (D) 6 h.

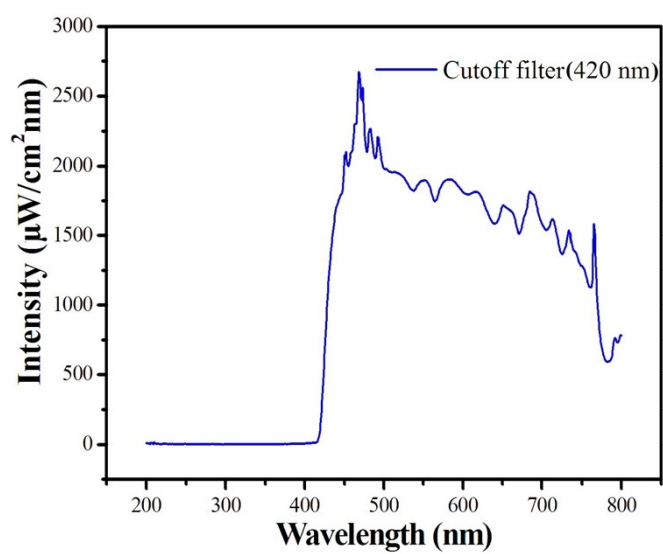


**Fig. S6.** The intensity and spectral distribution of the light source employed in the degradation experiments.

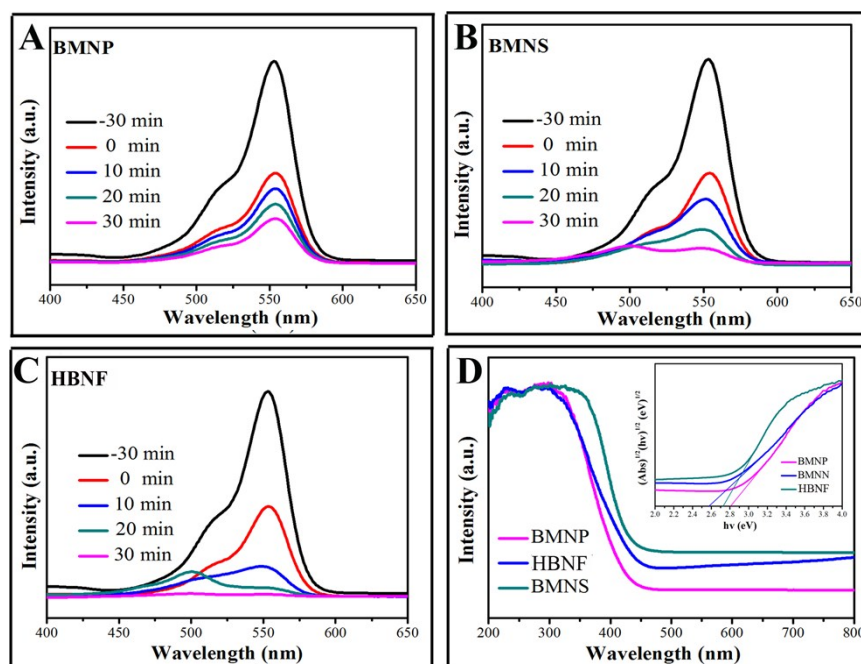


**Fig. S7.** Time-dependent optical absorption spectra of RhB ( $1.0 \times 10^{-5}$  M, 20 ml) degradation over the BMNP (A), BMNS (B) and HBNF (C) as photocatalysts and the UV-vis spectra of the corresponding photocatalysts (D).

Optical absorption of the HBNF, BMNS and BMNP were characterized by UV-vis technique and the obtained results are given in Fig. S7D. It is clearly that the samples all show a major absorption band between 370 nm and 510 nm and the steep shape of the absorption edge indicates a band-gap transition rather than the transition from the impurity level.<sup>6</sup> More specially, the band gap of the HBNF is estimated to be 2.58 eV from the onset of the absorption edge<sup>7</sup>, which is smaller than the BMNS's (2.72 eV) and BMNP's (2.81 eV).

#### Reference

6. T.F. Jaramillo, K.P. Jørgensen, J. Bonde, J.H. Nielsen, S. Horch, I. Chorkendorff, *Science*, 2007, **317**, 100–102.
7. T. Wu, G. Liu, J. Zhao, *J. Phys. Chem. B*, 1998, **102**, 5845–5851.

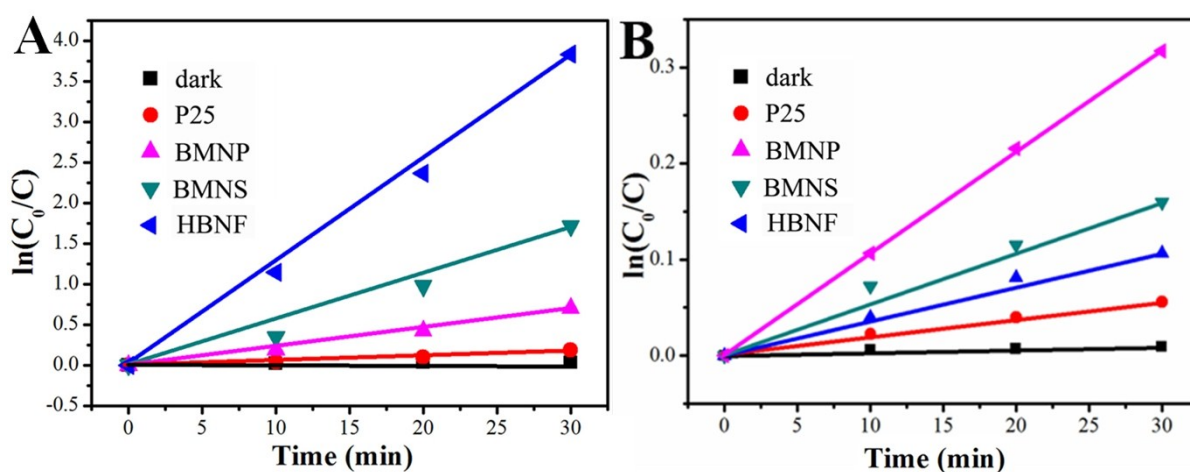


**Fig. S8.** The kinetics of photodegradation of RhB (A) and phenol (B) over different photocatalysts under visible-light irradiation.

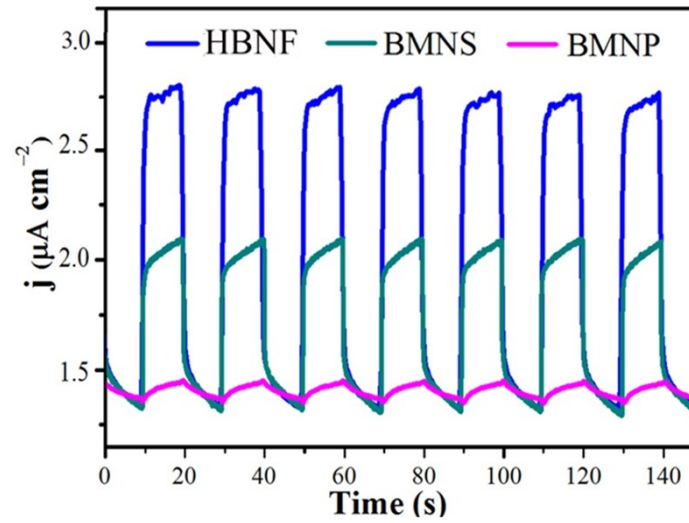


**Fig. S9.** Amperometric  $I-t$  curves of different  $\text{Bi}_2\text{MoO}_6$  samples under visible light illumination ( $\lambda > 420$  nm) in 0.1 M  $\text{Na}_2\text{SO}_4$ .